EBioMedicine 53 (2020) 102706

Contents lists available at ScienceDirect

EBioMedicine

journal homepage: www.elsevier.com/locate/ebiom

Research paper

Macrophage-derived myeloid differentiation protein 2 plays an essential role in ox-LDL-induced inflammation and atherosclerosis

Taiwei Chen[a,b,1], Weijian Huang[a,1], Jinfu Qian[a,b], Wu Luo[b], Peiren Shan[a], Yan Cai[c], Ke Lin[a,b], Gaojun Wu[a,*], Guang Liang[a,b,d,**]

[a] Department of Cardiology, the First Affiliated Hospital of Wenzhou Medical University, Wenzhou, Zhejiang, China
[b] Chemical Biology Research Center, School of Pharmaceutical Sciences, Wenzhou Medical University, Wenzhou, Zhejiang, China
[c] The Affiliated Cangnan Hospital, Wenzhou Medical University, Wenzhou, Zhejiang, China
[d] Zhuji Biomedicine Institute, School of Pharmaceutical Sciences, Wenzhou Medical University, Zhuji, Zhejiang, China

ARTICLE INFO

Article History:
Received 27 January 2020
Revised 20 February 2020
Accepted 21 February 2020
Available online xxx

Keywords:
Myeloid differentiation-2
Oxidized-LDL
Toll-like receptor 4
Atherosclerosis
Inflammation
Macrophages

ABSTRACT

Background: Atherosclerosis is a chronic inflammatory disease. Although Toll-like receptor 4 (TLR4) has been involved in inflammatory atherosclerosis, the exact mechanisms by which oxidized-low-density lipoproteins (ox-LDL) activates TLR4 and elicits inflammatory genesis are not fully known. Myeloid differentiation factor 2 (MD2) is an extracellular molecule indispensable for lipopolysaccharide recognition of TLR4.
Method: $Apoe^{-/-}Md2^{-/-}$ mice and pharmacological inhibitor of MD2 were used in this study. We also reconstituted $Apoe^{-/-}$ mice with either $Apoe^{-/-}$ or $Apoe^{-/-}Md2^{-/-}$ marrow-derived cells. Mechanistic studies were performed in primary macrophages, HEK-293T cells, and cell-free system.
Finding: MD2 levels are elevated in atherosclerotic lesion macrophages, and MD2 deficiency or pharmacological inhibition in mice reduces the inflammation and stunts the development of atherosclerotic lesions in $Apoe^{-/-}$ mice fed with high-fat diet. Transfer of marrow-derived cells from *Apoe-Md2* double knockout mice to *Apoe* knockout mice confirmed the critical role of bone marrow-derived MD2 in inflammatory factor induction and atherosclerosis development. Mechanistically, we show that MD2 does not alter ox-LDL uptake by macrophages but is required for TLR4 activation and inflammation via directly binding to ox-LDL, which triggers MD2/TLR4 complex formation and TLR4-MyD88-NFκB pro-inflammatory cascade.
Interpretation: We provide a mechanistic basis of ox-LDL-induced macrophage inflammation, illustrate the role of macrophage-derived MD2 in atherosclerosis, and support the therapeutic potential of MD2 targeting in atherosclerosis-driven cardiovascular diseases.
Funding: This work was supported by the National Key Research Project of China (2017YFA0506000), National Natural Science Foundation of China (21961142009, 81930108, 81670244, and 81700402), and Natural Science Foundation of Zhejiang Province (LY19H020004).

1. Introduction

Atherosclerosis leading to cardiovascular diseases is a significant driver of morbidity and mortality worldwide [1]. Atherosclerosis is typically seen alongside other cardiovascular comorbidities such as diabetes mellitus, metabolic syndrome, dyslipidemia, and hypertension [2]. The central process in atherosclerosis is dysregulated lipid metabolism and a maladaptive immune response. The process is initiated by vascular endothelial cell activation and damage [3,4]. Vascular damage causes subendothelial accumulation of low-density lipoproteins (LDL). Apolipoprotein B100 (ApoB100) of LDL binds to negatively charged extracellular proteoglycans facilitating retention [5,6]. Retained LDL is susceptible to oxidative modification by reactive oxygen species (ROS) and redox enzymes and facilitates the infiltration of monocytes [7,8]. Formation of macrophage-like foam cells loaded with lipids and successive accumulation of apoptotic cells, debris, and cholesterol crystals forms a necrotic core. In advanced stages, atherosclerotic plaques rupture and the disease manifests as acute coronary syndrome, myocardial infarction or stroke.

Critical to the development as well as the progression of atherosclerosis, is the interaction between macrophages and ox-LDL. This

* Corresponding author: Department of Cardiology, the First Affiliated Hospital of Wenzhou Medical University, Wenzhou, Zhejiang, China.
** Corresponding author at: Chemical Biology Research Center, School of Pharmaceutical Sciences, Wenzhou Medical University, Wenzhou, Zhejiang, China.
E-mail addresses: 2855930357@qq.com (G. Wu), wzmcliangguang@163.com (G. Liang).
[1] These authors contribute equally to this paper.

https://doi.org/10.1016/j.ebiom.2020.102706

Research in context

Evidence before this study

Atherosclerosis is a significant driver of cardiovascular diseases. Critical to the development of atherosclerosis is the interaction between macrophages and ox-LDL, which facilitates uptake of ox-LDL in macrophages and inflammatory activation. Myeloid differentiation 2 (MD-2) and Toll-like receptor 4 (TLR4) are a pair of recognition receptors of lipopolysaccharide in innate immune response. Recent studies have linked TLR4 in ox-LDL-induced inflammation and atherosclerosis. TLR4 has been shown to be essential for ox-LDL-induced macrophage inflammation and differentiation into foam cells. However, the exact mechanisms by which ox-LDL elicits TLR4-mediated inflammatory activation are not fully known. In addition, the role of macrophage MD2 in the progression of inflammatory atherosclerosis is unclear

Added value of this study

In this study, we investigated the role of MD2 in engaging TLR4 to drive atherosclerosis development. We show that MD2 does not participate in ox-LDL uptake by macrophages but is critical for ox-LDL-induced TLR4 activation and inflammatory cytokine expression. oxLDL may directly bind MD2 to induce MD2/TLR4 complex formation and inflammatory genesis in macrophages. MD2 deficiency and functional blockade in mice reduced atherosclerotic lesions. Transfer of marrow-derived cells from ApoE-MD2 double knockout mice to ApoE knockout mice showed that macrophage-derived MD2 in critical to atherosclerosis development.

Implications of all the available evidence

Our results shed new light on the role of MD2 in atherosclerosis and provide a mechanistic basis for ox-LDL-induced inflammatory responses. We also showed that pharmacological inhibition of MD2 by a small-molecule inhibitor prevented inflammatory macrophage activation and atherosclerosis development in ApoE$^{-/-}$ mice fed a HFD. Therefore, targeting MD2 may be a viable option to curb atherosclerosis. These data support the therapeutic potential of MD2 inhibitors in atherosclerosis-driven cardiovascular diseases.

interaction facilitates uptake of ox-LDL in macrophages and inflammatory activation [9]. However, the exact mechanisms by which ox-LDL elicits inflammatory activation and induces inflammatory genesis in macrophages are not fully known. Many studies have shown lesional macrophages express toll-like receptors (TLRs), a type of pattern recognition receptors (PRRs) mediating inflammatory activation [10]. Of the TLRs expressed on macrophages, TLR4 has been shown to be essential for ox-LDL-induced macrophage inflammation and differentiation into foam cell [11,12]. Apolipoprotein E (ApoE) knockout mice deficient in TLR4 also exhibit decreased development of atherosclerotic lesions, which is associated with significantly reduced inflammation [13,14]. Despite these promising studies, however, the precise mechanism underlying ox-LDL-induced TLR4 activation in macrophages involved in atherosclerosis remain unknown.

Upon binding to a ligand, TLRs dimerize and are activated [15,16]. In the case of TLR4 in pathogen-associated innate immunity, ligand (*e.g.* lipopolysaccharides) binding and activation requires a co-receptor protein myeloid differentiation factor 2 (MD2). MD2 is an extracellular molecule indispensable for LPS recognition of TLR4. TLR4 activation then causes recruitment of adaptor proteins such as myeloid differentiation primary-response protein 88 (MyD88), which triggers activation of multiple downstream signaling pathways, in particular nuclear factor-κB (NF-κB) to up-regulate a host of pro-inflammatory molecules [17,18]. However, the role of MD2 in ox-LDL-induced inflammation and atherosclerosis is unknown.

In this study, we investigated the role of MD2 in engaging TLR4 to drive atherosclerosis development. We show that MD2 does not participate in ox-LDL uptake by macrophages but is critical for ox-LDL-induced TLR4 activation and inflammatory cytokine expression. oxLDL may directly bind MD2 to induce MD2/TLR4 complex formation and inflammatory genesis in macrophages. MD2 deficiency and functional blockade in mice reduced atherosclerotic lesions. Results presented in here show that MD2 plays an important role in inflammatory induction in atherosclerosis. Targeting MD2 may be a viable option to curb atherosclerosis.

2. Materials and methods

2.1. Reagents

Low-density lipoproteins (LDL) and oxidized LDL (ox-LDL) were purchased from Peking Union-Biology (Beijing, China). DiI (3,3′-dioctadecylindocarbocyanine)-labeled ox-LDL was obtained from Yiyuan Biomedical Technologies (Guangzhou, China). LDL uptake inhibitor Dynasore [19] was purchased from Sigma-Aldrich (St. Louis, MO), and used at 80 μM as described previously for macrophages [20]. Oil Red O stain was obtained from Jiancheng Bioengineering Institute (Nanjing, China). MD2 antibody was from eBioscience (eBioscience, San Diego, CA). Antibodies against GAPDH and nuclear factor-κB (NF-κB) p65 subunit were obtained from Cell Signaling Technology (Danvers, MA). Antibodies against TLR4, myeloid differentiation primary response 88 (MyD88), smooth muscle actin (α-SMA), macrophage marker CD68, and Alexa-488 and −647-conjugated secondary antibodies were obtained from Abcam (Cambridge, MA). ApoB100 antibody was from Proteintech (Rosemont, USA). Antibody against Flag and HA tags were obtained from Sigma-Aldrich. Secondary horseradish peroxidase-conjugated antibodies for immunoblotting were purchased from Santa Cruz Biotechnology. NF-κB reporter plasmid (p-LV-NFκB-RE-EGFP) was purchased from Jiancheng Bioengineering Institute (Nanjing, China). Recombinant human MD2 protein was obtained from R&D Systems (Minneapolis, MN, USA). The small molecule MD2 inhibitor, (E)-3-(2,6-difluorophenyl)-1-(4-methoxyphenyl) prop-2-en-1-one (L6H9), was synthesized by our group and prepared to a purity of 99.2% as described previously [21]. L6H9 was dissolved in dimethylsulphoxide for *in vitro* studies and 1% sodium-carboxymethyl cellulose (CMC—Na) for *in vivo* administration.

2.2. Macrophage culture

Mouse primary peritoneal macrophages were isolated as described previously [22,23]. Briefly, mice received a single intraperitoneal injection of 6% thioglycollate solution (0.3 g beef extract, 1 g tryptone, 0.5 g sodium chloride dissolved in 100 mL ddH_2O, filtrated through 0.22-μm filter membrane). Two days later, mice were euthanized, and peritoneal cavity was flushed with RPMI-1640 medium (Gibco/BRL life Technologies, Eggenstein, Germany). Samples were centrifuged, and cell suspension was plated in RPMI-1640 medium containing 10% fetal bovine serum (Hyclone, Logan, UT), 100 U/mL penicillin, and 100 mg/mL streptomycin. Nonadherent cells were removed 2 h after seeding the cell suspension. A transfectable macrophage-like cell line derived from Balb/c mice, RAW264.7, was purchased from the Shanghai Institute of Biochemistry and Cell Biology (Shanghai, China). RAW264.7 cells maintain properties of macrophages including nitric oxide production, phagocytosis, and sensitivity to TLR agonists. RAW264.7 cells in this study were cultured in the same media as primary macrophages and used for studies involving

cell transfections. All ox-LDL exposures were carried out in cells at 50 μg/mL.

To measure cytokine production in cells, macrophages were exposed to ox-LDL at 50 μg/mL. Cell culture media was collected, and cells were pelleted. The levels of tumor necrosis factor alpha (TNF-α) and interleukin-6 (IL-6) in the media were detected using commercial ELISA kits (eBioScience, San Diego, CA). The level of cytokines in the media was normalized to the total protein levels of viable cell pellets. Under similar conditions, RNA was extracted to measure cytokine mRNA levels via real-time qPCR assay. Where indicated, L6H9 pretreatments were carried out for 1 h prior to ox-LDL exposure.

2.3. ox-LDL uptake assay

For uptake detection, macrophages were incubated 50 μg/mL DiI-ox-LDL for 3 h at 37 °C. Cells were washed with PBS and imaged using Leica TCS SP8 confocal laser scanning microscope (Buffalo Grove, USA). Cells under identical conditions were also dislodged and analyzed by flow cytometry (FACScalibur, Becton Dickinson, San Diego, CA, USA). The results of flow cytometry were expressed as mean fluorescence intensity after subtracting auto-fluorescence of cells (absence of DiI-ox-LDL).

For Oil Red O staining in primary macrophages, cells were incubated with 50 μg/mL ox-LDL for 24 h. Cells were then fixed in 4% paraformaldehyde for 15 min, washed with PBS, and incubated with a 0.5% working solution of Oil Red O for 15 min. Images were captured using Nikon microscope equipped with a digital camera (Tokyo, Japan).

2.4. Real-time quantitative polymerase chain reaction (qPCR)

Total RNA was extracted from cells and aorta tissues with TRIZOL (Thermo Fisher, Carlsbad, CA). Reverse transcription was carried out using PrimeScript RT Reagent Kit with gDNA Eraser (TAKARA, Japan). Quantitative PCR was conducted using iQ™ SYBR Green Supermix (Bio-Rad, Shanghai, China) in QuantStudio™ 3 Real-Time PCR System (Thermo Fisher). Primers were obtained from Thermo Fisher. Primer sequences used in this paper are listed in Supplementary Table S1.

2.5. Western blots and co-immunoprecipitation

Total protein from cells and tissues were extracted using lysis buffer (AR0101/0103, Boster Biological Technology Co. Ltd, Pleasanton, CA). Proteins were separated using 10% SDS-PAGE and then transferred to polyvinylidene fluoride membranes. Before adding specific primary antibodies, membranes were blocked in Tris-buffered saline (pH 7.4, containing 0.05% Tween 20 and 5% non-fat milk) for 1.5 h at room temperature. Protein bands were then detected by incubating with horseradish peroxidase-conjugated secondary antibodies and enhanced chemiluminescence reagent (Bio-Rad). Band densities were quantified using Image J software (Version 1.38e, NIH, Bethesda, MD) and normalized to loading controls.

For co-immunoprecipitation assays, cell extracts prepared following treatments were incubated with indicated antibodies overnight at 4 °C, and immunoprecipitated with protein G-sepharose beads at 4 °C for 2 h. Immunoprecipitation samples were further subjected to immunoblotting for the detection of co-precipitated proteins. Total lysates were also performed for western blot analysis as an input control. Protein interactions were quantified using Image J (NIH).

2.6. TLR4 signaling protein expression

Human embryonic kidney (HEK) 293T cells were obtained from the Shanghai Institute of Biochemistry and Cell Biology (Shanghai, China). HEK-293T cells were cultured in DMEM supplemented with 25 mM of D-glucose, 10% fetal bovine serum, 100 U/mL penicillin, and 100 U/mL streptomycin. To assess TLR4 dimerization upon ox-LDL exposure, HEK-293 cells were transfected with pCMV-HA-TLR4, pCMV-Flag-TLR4 and pCMV-His-MD2 (Sino Biological) using polyethylenimine (PEI; Sigma-Aldrich). MD2-TLR4 and MyD88-TLR4 interaction in HEK-293T cells was assessed similarly. Cells were transfected with pCMV-His-MD2 and -Flag-TLR4 or pCMV-Flag-MyD88, -HA-TLR4, and −His-MD2 plasmids (all plasmids were obtained from Sino Biological).

2.7. Generation of stable NF-κB EGFP RAW264.7 cells

RAW264.7 cells were transfected with pGL3-NF-κB-EGFP lentiviral particles to obtain stable cells expressing NF-κB reporter. Briefly, lentivirus containing the response element of NF-κB was first generated by co-transfecting HEK-293T cells with p-LV-NFκB-RE-EGFP (Inovogen) and packaging plasmids (psPAX2 and pMD2.G) using PEI. Supernatant was collected 48 h later and filtered using a 0.45 μm filter. Then, RAW264.7 cells were incubated with supernatant and 8 μg/mL polybrene (Sigma-Aldrich) for 12 h. Cells were selected with 2 μg/mL puromycin (Invitrogen, San Diego). Following transfection, cells were challenged with 50 μg/mL ox-LDL or LDL for 6 h. Mean fluorescence intensity was analyzed by flow cytometry.

2.8. MD2 binding assay

The direct binding of ox-LDL with rhMD2 was determined by cell-free ELISA. rhMD2 protein (2 μg/mL) was immobilized to ELISA microplate surface. Then DiI-labelled ox-LDL (50 μg/mL) was added and incubated for 2 h. After rinsing, the fluorescence value of each well was detected using spectraMax M5 (Molecular Devices, Sunnyvale, CA). The results of measurements are expressed as relative fluorescence intensity (RFI) after subtracting background fluorescence of empty wells (absence of DiI-Ox-LDL).

2.9. Mouse model of atherosclerosis

All protocols involving animal experiments were approved by the Wenzhou Medical University Animal Policy and Welfare Committee (Approved documents: wydw2017−0804) and adhered to the NIH guidelines (Guide for the care and use of laboratory animals). For our studies, we utilized the hypercholesterolemic apolipoprotein E-deficient (*Apoe*$^{-/-}$) model which recapitulates disease initiation and progression [5,24]. *Apoe*$^{-/-}$ mice on C57BL/6 background were obtained from Jackson Laboratory (Cat No. 002052). *Md2*$^{-/-}$ mice (B6.129P2-Ly96 KO) on C57BL/6 background were provided by Riken BioResource Center of Japan (Tsukuba, Ibaraki, Japan). No phenotypic abnormality in MD-2 KO mice was observed under the baseline condition. *Apoe*$^{-/-}$ mice were crossed with *Md2*$^{-/-}$ mice for at least 6 generations to generate *Apoe*$^{-/-}$*Md2*$^{-/-}$ mice. To model the development of atherosclerosis, *Apoe*$^{-/-}$*Md2*$^{-/-}$ mice and age-matched *Apoe*$^{-/-}$ mice (18−20 g, 8-week-old, n = 6 mice per group) were fed a high-fat diet (HFD) containing 60 kcal.% fat, 20 kcal.% protein and 20 kcal.% carbohydrate (HFK Bioscience Co. Ltd.; Cat. #MD12033) for 16 weeks.

For studies involving MD2 inhibitor L6H9, *Apoe*$^{-/-}$ mice were fed a HFD for 8 weeks and then were divided into two groups: HFD and HFD+L6H9. L6H9 reconstituted in 1% CMC—Na solution was administered by oral gavage at 10 mg/kg every 2 days. The HFD group received 1% CMC—Na solution alone. Mice were maintained on HFD for an additional 8 weeks (n = 6 mice per group).

Body weights were recorded weekly. At the end of the study, animals were euthanized under sodium pentobarbital anesthesia and the blood was collected. Aortas were fixed in 4% paraformaldehyde or snap-frozen in liquid nitrogen. The levels of serum lipids including total triglycerides (TG), total cholesterol (TCH), low-density

lipoprotein (LDL), and high-density lipoprotein (HDL) were measured by respective assay kits obtained from Nanjing Jiancheng (Jiangsu, China).

In addition, C57BL/6 wildtype mice, *Md2*$^{-/-}$ mice, and *Tlr4*$^{-/-}$ mice (B6.B10ScN-Tlr4$^{lps\text{-}del}$/JthJ; Stock #007227) [25] were used for isolation of mouse primary peritoneal macrophages as described above.

2.10. Bone marrow transplantation

One week before transplantation, *Apoe*$^{-/-}$ mice were put in filter-top cages and given acidified water containing neomycin (1.1 mg/L) and polymyxin B sulphate (1000 U/L). 12 h prior to transplantation, mice were subjected to total body irradiation (6 Gy). For transplantation, *Apoe*$^{-/-}$ mice were injected intravenously with 5×10^6 bone marrow cells from pools of bone marrow from *Apoe*$^{-/-}$ mice (KO→KO group) or *Apoe*$^{-/-}$*Md2*$^{-/-}$ mice (DKO→KO gourp). Tail clip samples and peritoneal macrophages were used for genotyping and confirmation of reconstitution. Mice were then fed a HFD for 16 weeks to assess the development of atherosclerotic lesions.

2.11. Atherosclerotic lesion analysis

For en face lesion analysis of the aorta, whole aorta and aortic sinus were dissected out, opened longitudinally from heart to the iliac arteries, and stained with Oil Red O. The heart and proximal aorta were collected and embedded in optimum cutting temperature compound for quantification of plaque lesion. Serial 5 μm-thick cryosections of aortic sinus from each mouse were obtained. Sections were stained with Oil Red O and hematoxylin for analysis of plaque sizes. Paraffin-embedded sections were used for Masson Trichrome staining. Frozen sections were used for CD68, α-SMA, MD2, and apoB100 staining. For immunofluorescence staining, slides were fixed in cold methanol and permeabilized using 0.3% Triton-X. Then, slides were blocked using 5% bovine serum albumin for 30 min and incubated overnight with primary antibodies (1:500). Alexa-488/647 conjugated secondary antibodies (Abcam, 1:500) were used for detection. The isotype antibodies were used as controls. Slides were counterstained with DAPI.

2.12. Human specimens

All the procedures involving human samples were approved by the First Affiliated Hospital of Wenzhou Medical University in China and all samples were obtained with informed consent (the Ethical Approval Number 2018-153). Fresh blood samples were obtained from healthy volunteers (NP, $n = 15$) and patients diagnosed with coronary artery disease (AS, $n = 40$). The baseline characteristics of healthy NP and AS patients were shown in Supplementary Table S2. Peripheral blood mononuclear cells were prepared using Human Whole Blood Mononuclear Cell Separation Solution (Solarbio, China). mRNA and proteins were extracted from cells and subjected to MD2 level determination. Serum prepared from blood samples was used for TNF-α and MD2 ELISA (eBioscience, San Diego, CA)

2.13. Statistical analysis

All experiments were randomized and blinded. In all *in vitro* experiments, data represented at least 3 independent experiments and expressed as means ± SEM. In *in vivo* experiments, data were expressed as mean ± SEM, except body weight data. Statistical analyses were performed with GraphPad Pro Prism 7.00 (GraphPad, San Diego, CA, USA). The exact group size (n) for each experimental group/condition is provided and 'n' refers to independent values, not replicates. The statistical significance of differences between two groups was determined by Student's t tests. One-way ANOVA followed by multiple comparisons test with Bonferroni correction was employed to analyze the differences for more than two groups. *P* value < 0.05 was considered statistically significant (in all figures: *, $p < 0.05$; **, $p < 0.01$; *** $p < 0.001$; ns = not significant).

3. Results

3.1. Increased MD2 in atherosclerotic lesions from mice and in peripheral-blood mononuclear cells from patients with coronary arteriosclerotic disease

Our first objective was to determine whether levels of MD2 are associated with atherosclerotic injury. To achieve this, we assessed MD2 protein levels in aortas of *Apoe*$^{-/-}$ mice maintained on a high-fat diet (HFD). This HFD-induced model of atherosclerosis reliably recapitulates the early events in atherosclerosis pathogenesis [26,27]. We found a remarkable increase in the amount of MD2 in aortas harvested from mice fed a HFD compared to the normal/low-fat diet (Fig. 1a and b). MD2 also exists as a soluble form (sMD2) found in the circulation which appears important for sensing endogenous ligands [28]. Increased levels of sMD2 protein were also found in blood samples from mice fed a HFD (Fig. 1c) and positively associated with levels of circulating inflammatory cytokine tumor necrosis factor-α (TNF-α; Fig. 1d). Immunofluorescence staining of cross-sectioned aortic sinus from mice fed a HFD showed that MD2 protein mostly localizes to CD68-positive macrophages (Fig. 1e, Supplementary Fig. S1a). We also found that ox-LDL incubation for 24 h significantly increased MD2 protein levels in mouse primary macrophages (Supplementary Fig. S1b). We know that following intimal injury, multiple factors may lead to phenotypic change in vascular smooth muscle cells from the quiescent state to the actively proliferating synthetic state. We stained the cross sections of aortic sinus for α-smooth muscle actin (α-SMA) to determine whether these cells also contribute to increased MD2 levels. Our results show that modest levels of α-SMA-positive cells were immunoreactive to MD2 (Fig. 1f, Supplementary Fig. S1a). These studies point to infiltrating macrophages as the primary source of increased MD2 protein in atherosclerotic lesions. By the way, lacking the immunofluorescence staining for endothelial cell marker here may be a limitation of this paper.

To explore whether increased MD2 levels found in the experimental model is biologically relevant, we isolated peripheral blood mononuclear cells from patients diagnosed with coronary artery disease (AS) and compared MD2 protein levels in the isolated cells to those obtained from age-matched healthy volunteers (NP). Our results show the levels of MD2 were elevated in circulating mononuclear cells from patients with atherosclerotic disease (Fig. 1g, and h). We also found increased circulating sMD2 and TNF-α in samples obtained from patients with atherosclerotic injury (Fig. 1i and j). These results show that increased macrophage-derived MD2 protein levels may be important in the progress of inflammatory atherosclerosis.

3.2. Diminished atherosclerotic injuries in MD2 knockout mice

Increased levels of MD2 in aortas of mice with atherosclerotic lesions prompted us to examine the effect of MD2 deficiency in the process. We crossed *Apoe*$^{-/-}$ mice with *Md2*$^{-/-}$ mice to generate *Apoe*$^{-/-}$*Md2*$^{-/-}$ double knockouts and compared them to *Apoe*$^{-/-}$ (Supplementary Figure S2). HFD feeding of *Apoe*$^{-/-}$ mice led to heterogenous plaque development along the aorta (Fig. 2a). Oil Red O staining showed significantly less plaques in ApoE$^{-/-}$MD2$^{-/-}$ compared to ApoE$^{-/-}$ mice. Aortic sinus stained with Oil Red O confirmed these observations and showed considerably less stained area in tissues harvested from *Apoe*$^{-/-}$*Md2*$^{-/-}$ mice (Fig. 2b). These beneficial changes caused by *Md2* knockout were seen despite no any differences in the body weights of mice (Supplementary Figure S3a) and

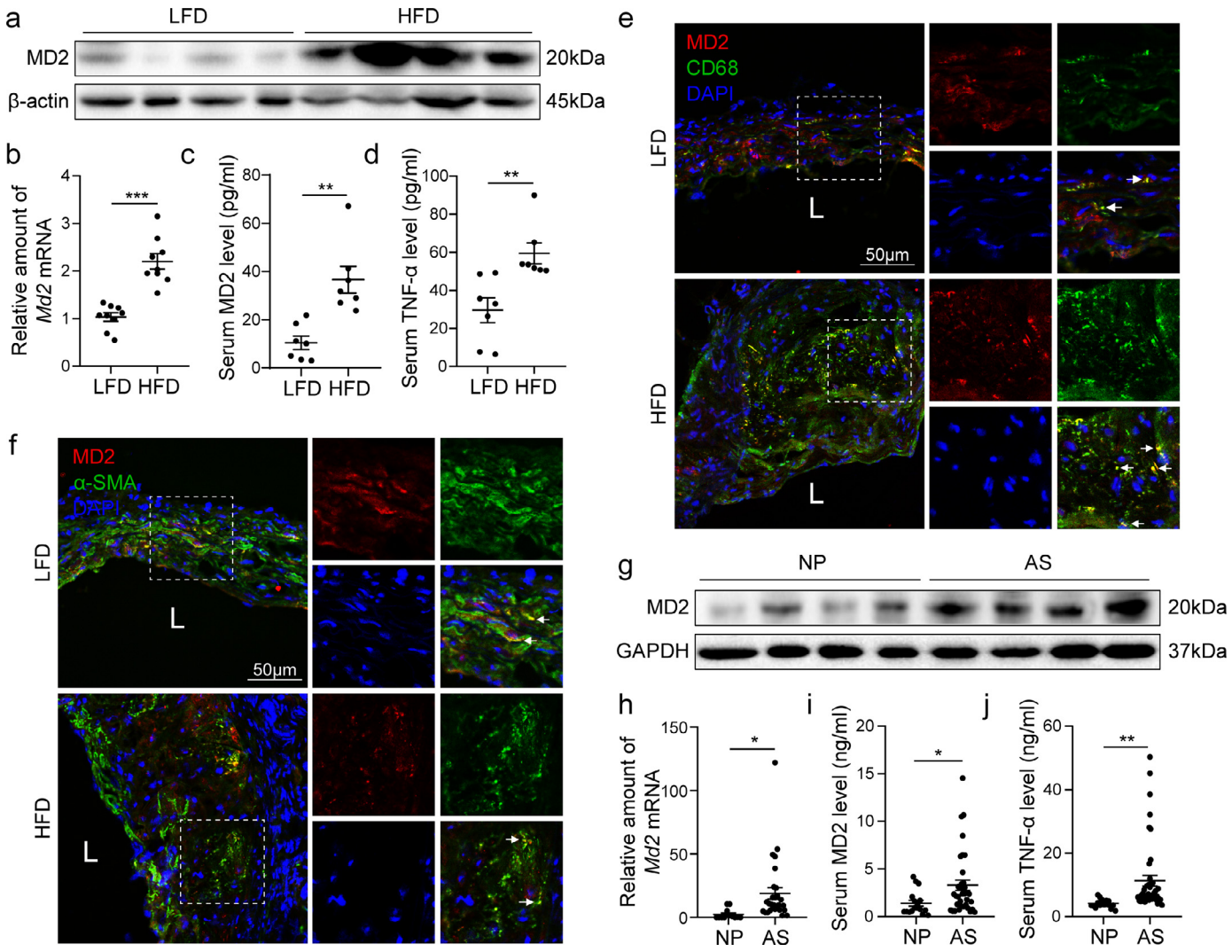

Fig. 1. MD2 is elevated in atherosclerotic lesion macrophages. (**a**) MD2 protein levels in aortas of *Apoe*$^{-/-}$ mice fed a high-fat diet (HFD) or normal/low-fat diet (LFD) were detected by western blotting. β-actin was used as loading control. Representative immunoblots were shown. (**b**) mRNA levels of *Md2* in aortic sinus of *Apoe*$^{-/-}$ mice fed with LFD and HFD [n = 9]. (**c, d**) Serum levels of soluble MD2 protein (c) and tumor necrosis factor-α (TNF-α; d) in *Apoe*$^{-/-}$ mice fed with LFD and HFD [n = 7]. (**e, f**) Representative immunofluorescence staining of MD2 (red, e and f), macrophage marker CD68 (green, e), and smooth muscle cell marker α-SMA (green, f). Tissues were counterstained with DAPI (blue). White arrows indicate co-location of MD2 and CD68 (e) or α-SMA (f) staining [scale bar = 50 μm]. (**g**) Western blot analysis of MD2 protein levels in human peripheral blood mononuclear cells (hPBMCs) isolated from patients with atherosclerosis (AS) and without AS (normal peoples, NP). (**h**) mRNA levels of *Md2* in hPBMCs. (**i, j**) Serum levels of MD2 protein (i) and tumor necrosis factor-α (TNF-α; j) in hPBMCs isolated from AS [n = 40] and NP [n = 15]. (For interpretation of the references to color in this figure legend, the reader is referred to the web version of this article.)

levels of serum triglycerides, total cholesterol, and LDL (Supplementary Fig. S3b). However, we did find elevated levels of HDL in *Apoe*$^{-/-}$*Md2*$^{-/-}$ mice compared to *Apoe*$^{-/-}$ mice (Supplementary Fig. S3b).

Immunostaining of aortic sinus sections showed lower immunoreactivity for α-SMA in *Apoe*$^{-/-}$*Md2*$^{-/-}$ mice compared to *Apoe*$^{-/-}$ mice, indicating less smooth muscle proliferation (Fig. 2c). Surprisingly, however, no differences were found in connective tissue deposition and fibrosis between the two groups (Fig. 2d). We next examined the levels of pro-inflammatory cytokines [29,30] and adhesion molecules [31,32], which are associated with atherosclerosis. We measured serum levels of TNF-α and IL-6 in mice and observed significantly higher levels in *Apoe*$^{-/-}$ mice maintained on HFD compared to *Apoe*$^{-/-}$*Md2*$^{-/-}$ mice (Fig. 2e). The mRNA levels of these cytokines in aortic sinus were also higher in *Apoe*$^{-/-}$ mice (Fig. 2f). In addition, mRNA levels of *Il-1β*, intercellular adhesion molecule-1 (*Icam-1*), and vascular cell adhesion molecule-1 (*Vcam-1*) showed a similar pattern of expression (Fig. 2f). These findings clearly show reduced inflammatory responses in aortas of HFD-fed *Apoe*$^{-/-}$*Md2*$^{-/-}$ mice, and perhaps suggest less macrophage infiltration. Immunostaining of aortic sinus for macrophage marker CD68 in tissues from *Apoe*$^{-/-}$*Md2*$^{-/-}$ and *Apoe*$^{-/-}$ mice confirmed this latter notion (Fig. 2g and h). Collectively, these studies show that MD2 deficiency protects against the development of atherosclerotic plaques, possibly through reduced macrophage infiltration and expression of inflammatory cytokines.

3.3. MD2 in bone marrow-derived cells plays a critical role in the development of atherosclerotic lesions

To examine the contribution of macrophage MD2 in mediating atherosclerotic injuries, we reconstituted *Apoe*$^{-/-}$ mice with either *Apoe*$^{-/-}$ (control KO→KO group) or *Apoe*$^{-/-}$*Md2*$^{-/-}$ (DKO→KO group) marrow-derived cells. Tail clip samples, isolated peritoneal macrophages, blood mononuclear cells, heats and aortas were used to confirm the desired combinations (Supplementary Figure S4). Mice were then maintained on HFD for 16 weeks and the development of atherosclerotic lesions was followed. We did not find any changes to body weight gain in mice fed a HFD following KO or DKO marrow cell reconstitution (Supplementary Figure S5a). The profiles of serum

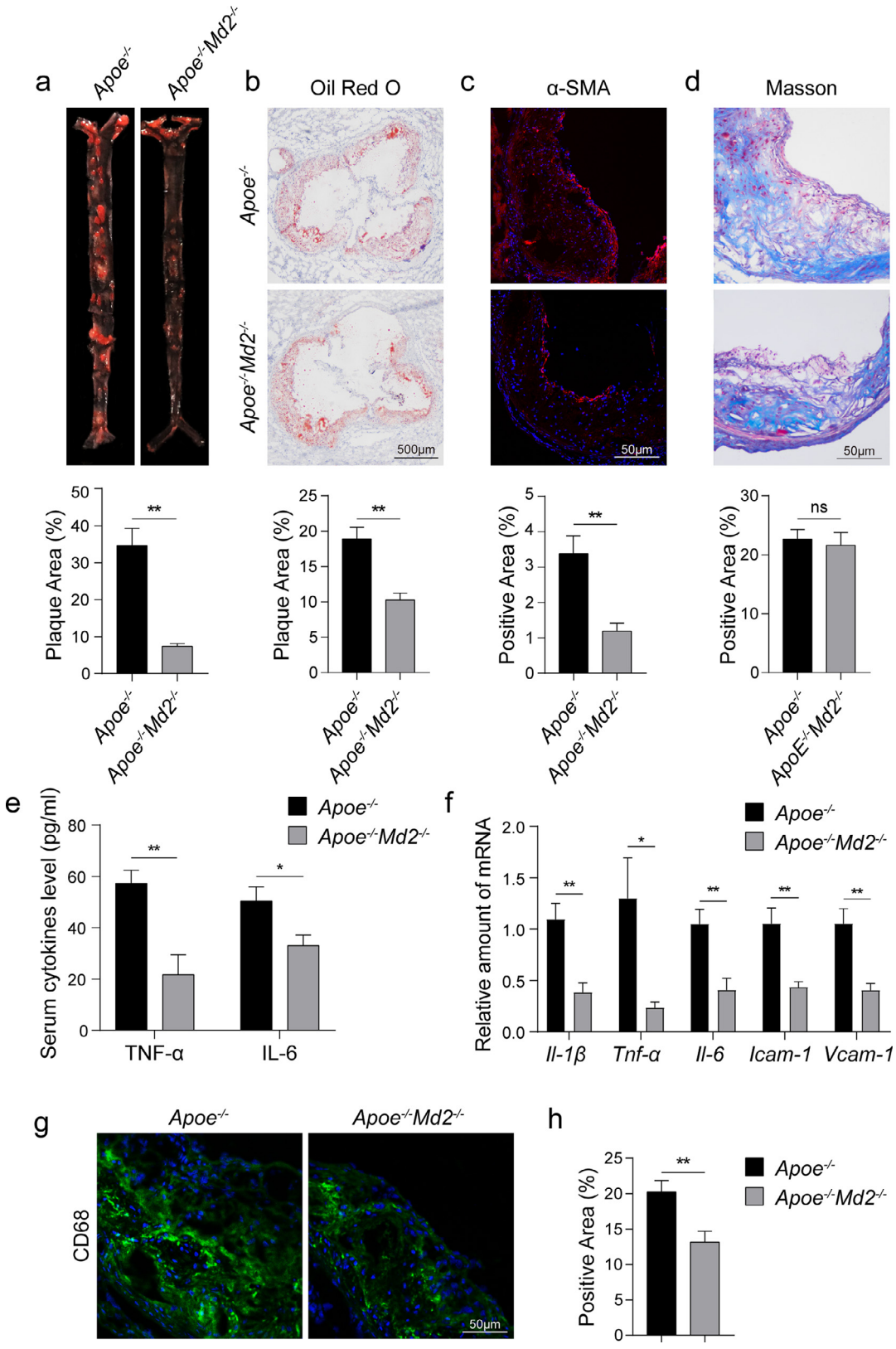

Fig. 2. MD2 deficiency reduces atherosclerosis in HFD-fed ApoE$^{-/-}$ mice. (**a**) En face Oil Red O staining of aortas from *Apoe*$^{-/-}$ and *Apoe*$^{-/-}$*Md2*$^{-/-}$ mice fed a HFD for 16 weeks. Oil Red O staining highlighting neutral lipids (red). Lower panel showing quantification of plaque lesion area from Oil Red O staining. Plaque area was defined as percentage of total surface area of the aorta [n = 6]. (**b**) Oil Red O staining of aortic sinus. Lower panel showing quantification of lesion area highlighted by Oil Red O staining [n = 6; scale bar = 500 μm]. (**c**) Representative images of α-SMA (red) staining of aortic sinus. Lower panel showing quantification of α-SMA staining area [n = 6; scale bar = 50 μm]. (**d**) Representative images of Masson's Trichome staining for collagen deposition. Lower panel showing quantification of fibrotic area [n = 6; scale bar = 50 μm]. (**e**) Serum levels of pro-inflammatory cytokines TNF-α and IL-6 in mice fed a HFD [n = 10]. (**f**) mRNA analysis of proinflammatory cytokines (*Il-1β*, *Tnf-α*, *Il-6*) and adhesion molecules (*Icam-1*, *Vcam-1*) in aortic sinus [n = 6]. (**g**) Representative immunofluorescence staining images for CD68 (green) in aortic sinus. Tissues were counterstained with DAPI (blue) [scale bar = 50 μm]. (**h**) Quantification of CD68-positive area in aortic sinus slices [n = 6]. (For interpretation of the references to color in this figure legend, the reader is referred to the web version of this article.)

levels of triglycerides, total cholesterol, LDL, and HDL in DKO→KO mice showed no significant difference with that in KO→KO mice (Supplementary Figure S5B). As expected, mice transplanted with DKO marrow cells showed reduced atherosclerotic plaques as evident through Oil Red O staining (Fig. 3a and b). α-SMA immunoreactivity was also lower in DKO→KO mice (Fig. 3c). No differences were seen in connective tissue deposition (Fig. 3d). Similarly, macrophage MD2 deficiency showed reduced inflammatory factor expression (Fig. 3eand f) and CD68-reactivity in aortic sinus of mice (Fig. 3g and h) in HFD-fed DKO→KO mice. These results strongly support the notion that MD2 in bone marrow−derived hematopoietic cells is critical for atherosclerotic plaque formation and inflammatory signaling in lesions.

3.4. MD2 mediates ox-LDL-induced proinflammatory cytokine production and NF-κB activation

Since the interaction between ox-LDL and macrophages is essential for inflammatory macrophage activation [9], we tested the possibility the MD2 deficiency perhaps alters this process. To test the role of MD2, we harvested peritoneal macrophages from wildtype and *Md2*$^{-/-}$ mice and exposed these cells to ox-LDL in culture to assess activation. Ox-LDL increased *Tnf-α* and *Il-6* mRNA expression and cytokine production in cells isolated from wildtype mice but not in cells from *Md2*$^{-/-}$ mice (Fig. 4a and b). We also found that this induction of inflammatory factors was specific to ox-LDL, as exposure of wildtype macrophages to unmodified-LDL was not associated with increased cytokine production (Supplementary Figure S6a). We then examined the activation of NF-κB, a downstream transcription factor of MD2/TLR4 signaling in innate immunity, which regulates the expression of inflammatory cytokines [33−35]. We firstly measured the levels of inhibitor of κB (IκBα) which keeps NF-κB activity in check. IκBα levels were significantly deceased in wildtype macrophages exposed to ox-LDL, indicating activation of NF-κB (Fig. 4c). In contrast, no changes in IκBα were found in *Md2*$^{-/-}$-derived macrophages upon ox-LDL exposure (Fig. 4c). This finding was then confirmed by NF-κB p65 immunoblotting using nuclear protein fractions prepared from the cells. Fig. 2d shows increased nuclear NF-κB p65 proteins only in cells harvested from wildtype mice but not from *Md2*$^{-/-}$ mice. The staining analysis of NF-κB p65 subunit in cultured macrophages from wildtype and *Md2*$^{-/-}$ mice also shows that ox-LDL increases nuclear immunoreactivity to NF-κB p65 only in wildtype macrophages (Fig. 4e). Finally, we transfected mouse RAW264.7 macrophages with reporter plasmid for NF-κB transcriptional activity. Exposure of transfected macrophage line to ox-LDL, but not native LDL, increased NF-κB activity (Supplementary Figure S6b). These data on NF-κB activity are consistent with the observed profile of inflammatory cytokines.

3.5. MD2 is essential for ox-LDL-induced TLR4 dimerization and activation

We next examined the potential mechanisms by which MD2 deficiency prevents ox-LDL-induced inflammation in macrophage. As a PRR, TLR4 and its assistant protein MD2 are proteins in cell surface. In innate immunity, LPS stimulates the formation of MD2/TLR4 complex to recruit MyD88 to generate pro-inflammatory molecules. We then examined whether ox-LDL directly initiates MD2/TLR4 complex formation and MyD88 recruitment. Our results show that exposure of macrophages from wildtype mice to ox-LDL increases the association of MD2 with TLR4 in a short-time duration (Fig. 5a). Peak interaction was seen at 30 min post-exposure and was maintained for at least 60 min. This enhanced MD2-TLR4 interaction by ox-LDL was confirmed in HEK-293T cells expressing MD2-His and TLR4-Flag (Fig. 5b). Then, we examined TLR4 dimerization by ox-LDL. We know that MD2-mediated TLR4 activation requires dimerization of two TLR4 receptor chains [36]. Therefore, we transfected plasmids encoding HA-TLR4 and Flag-TLR4 in HEK-293T cells. Transfected cells were then exposed to ox-LDL for 30 min with or without MD2-His plasmid transfection. Our results show that ox-LDL causes TLR4 dimerization in the presence of MD2 (Fig. 5c). To assess the effect of MD2 on ox-LDL-induced interaction between TLR4 and its downstream adapter MyD88, we isolated primary macrophages from widetype and *Md2*$^{-/-}$ mice. Data in Fig. 5d show that TLR4 associates with MyD88 following ox-LDL exposure only in wildtype macrophages and not in *Md2*$^{-/-}$ cells. HEK-293T cells expressing TLR4-HA and MyD88-Flag also showed increased TLR4-MyD88 interaction, only in the presences of MD2-His expression and ox-LDL exposure (Fig. 5e). These results illustrate that MD2 is required for TLR4 activation by ox-LDL.

3.6. oxLDL may directly interact with MD2 protein and leads to MD2/TLR4 activation

It remains unclear how ox-LDL leads to MD2/TLR4 complex formation. It has been reported that saturated fatty acids, cholesterol, and oxidized phospholipids may directly bind to MD2 and activate MD2/TLR4 complex [37−39]. Since ox-LDL contains numerous saturated fatty acids, cholesterol, and oxidized phospholipids, we speculate that these elements may make ox-LDL directly interact with MD2 in cell surface. We first examined whether ox-LDL abrogated LPS-induced strong inflammation in macrophages. Results showed that, although ox-LDL alone induced about 5−10 fold increase in TNF-α and IL-6 production, ox-LDL reduced LPS-induced TNF-α and IL-6 production (Supplementary Fig. S7), indicating a possible interaction between ox-LDL and MD2. Since the major protein of ox-LDL is apolipoprotein B100 (ApoB100), we exposed primary macrophages harvested from wildtype mice to ox-LDL and examined ApoB100-MD2 interaction by co-immunoprecipitation. Our results show that exposure of macrophages to ox-LDL increases the formation of a complex comprising ApoB100-MD2-TLR4 (Fig. 5f). ApoB100 of unmodified LDL, however, did not enhance this complex formation (Fig. 5f). Similar results were observed in HEK-293T cells expressing TLR4-HA and MD2-His (Fig. 5g). Co-staining macrophages for MD2 and ApoB100 showed increased co-localization of the two proteins in cells upon exposure to ox-LDL (Fig. 5h). Consistent with our immunoprecipitation studies, however, LDL exposure did not generate co-localized MD2 and ApoB100 reactivity (Fig. 5h, Supplementary Fig. S8a). This suggests that ox-LDL may directly bind MD2 to induce MD2/TLR4 complex formation. We then exposed macrophages harvested from wildtype, *Tlr4*$^{-/-}$, and *Md2*$^{-/-}$ mice to ox-LDL. Interestingly, our data in Fig. 5i and j show that ApoB100 in ox-LDL binds to TLR4 and MD2 separately. Knockout TLR4 did not affect the interaction of ApoB100 with MD2 and *vice versa* (Fig. 5i and j). Although ox-LDL separately interacts with MD2 and TLR4, activation of TLR4 by ox-LDL requires the presence of MD2 protein (Fig. 5c−e). We then tested the possible direct interaction between ox-LDL and MD2 in cell-free system. We immobilized recombinant human MD2 protein (rhMD2) and added DiI-labeled ox-LDL. Our data shows an ox-LDL attachment in the presence of rhMD2 indicating possible direct interaction (Fig. 5k). Lastly, we stained aortic sinus sections from *Apoe*$^{-/-}$ mice fed a HFD to determine whether ApoB100 colocalizes with MD2 *in vivo*. Fig. 5l shows that HFD feeding was associated with increased co-localization of MD2 and ApoB100 in aortic sinus of mice. These results suggest that ox-LDL may directly associate with MD2 protein and initiate MD2-TLR4 inflammatory signaling. MD2 in macrophages is required for ox-LDL's pro-inflammatory responses.

3.7. MD2 in macrophages is not required for ox-LDL uptake

Macrophages are also essential for ox-LDL update in atherosclerosis [9]. We examined the role of MD2 in ox-LDL update in macrophages. We incubated wildtype and *Md2*$^{-/-}$ macrophages with DiI-

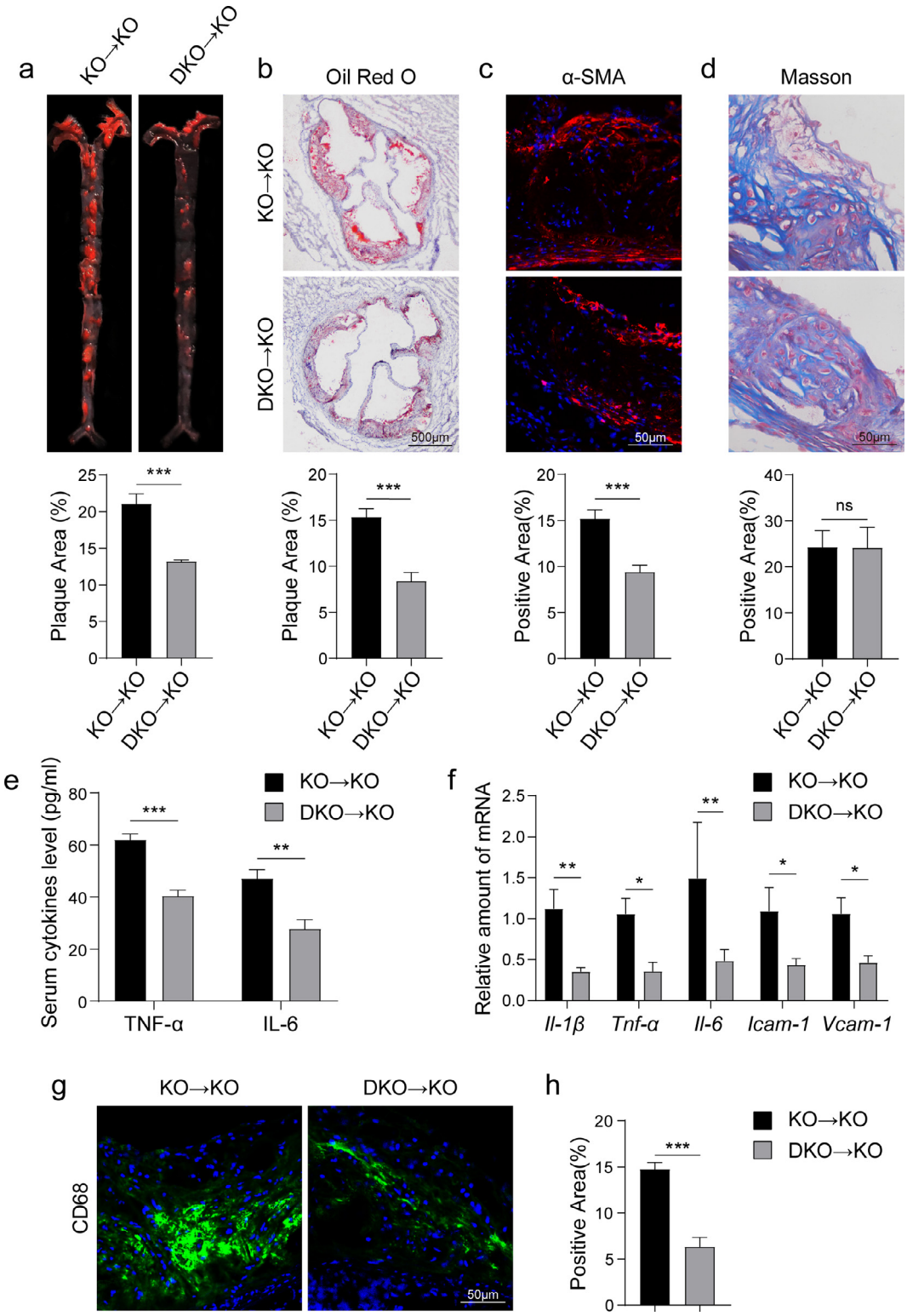

Fig. 3. Bone marrow-derived MD2 play a critical role in the development of atherosclerotic lesions *Apoe*$^{-/-}$ mice were irradiated and received bone marrow cells from either *Apoe*$^{-/-}$ mice or *Apoe*$^{-/-}$*Md2*$^{-/-}$ mice. KO→KO: marrow-derived cells from *Apoe*$^{-/-}$ (KO) mice were transplanted in irradiated *Apoe*$^{-/-}$ (KO) mice; DKO→KO: marrow-derived cells from *Apoe*$^{-/-}$*Md2*$^{-/-}$ (DKO) mice were transplanted in irradiated *Apoe*$^{-/-}$ (KO) mice. Mice were then fed a HFD for 16 weeks. (**a**) Oil Red O staining of aortas from mice transplanted with KO or DKO marrow cells. Lower panel showing quantification of plaque lesion area. [n = 6]. (**b**) Oil Red O staining of aortic sinus. Lower panel showing quantification of lesion area [n = 6; scale bar = 500 μm]. (**c**) Representative images of α-SMA (red) staining of aortic sinus. Lower panel showing quantification of α-SMA staining area [n = 6; scale bar = 50 μm]. (**d**) Representative images of Masson's Trichome staining of aortic sinus. Lower panel showing quantification of fibrotic area [n = 6; scale bar = 50 μm]. (**e**) Serum levels of TNF-α and IL-6 in mice (n = 8). (**f**) mRNA levels of inflammatory cytokines (*Il-1β*, *Tnf-α*, *Il-6*) and adhesion molecules (*Icam-1*, *Vcam-1*) in aortic sinus [n = 6]. (**g**) Representative immunofluorescence staining images for CD68 (green) in aortic sinus. Tissues were counterstained with DAPI (blue) [scale bar = 50 μm]. (**h**) Quantification of CD68-positive area in aortic sinus slices [n = 6]. (For interpretation of the references to color in this figure legend, the reader is referred to the web version of this article.)

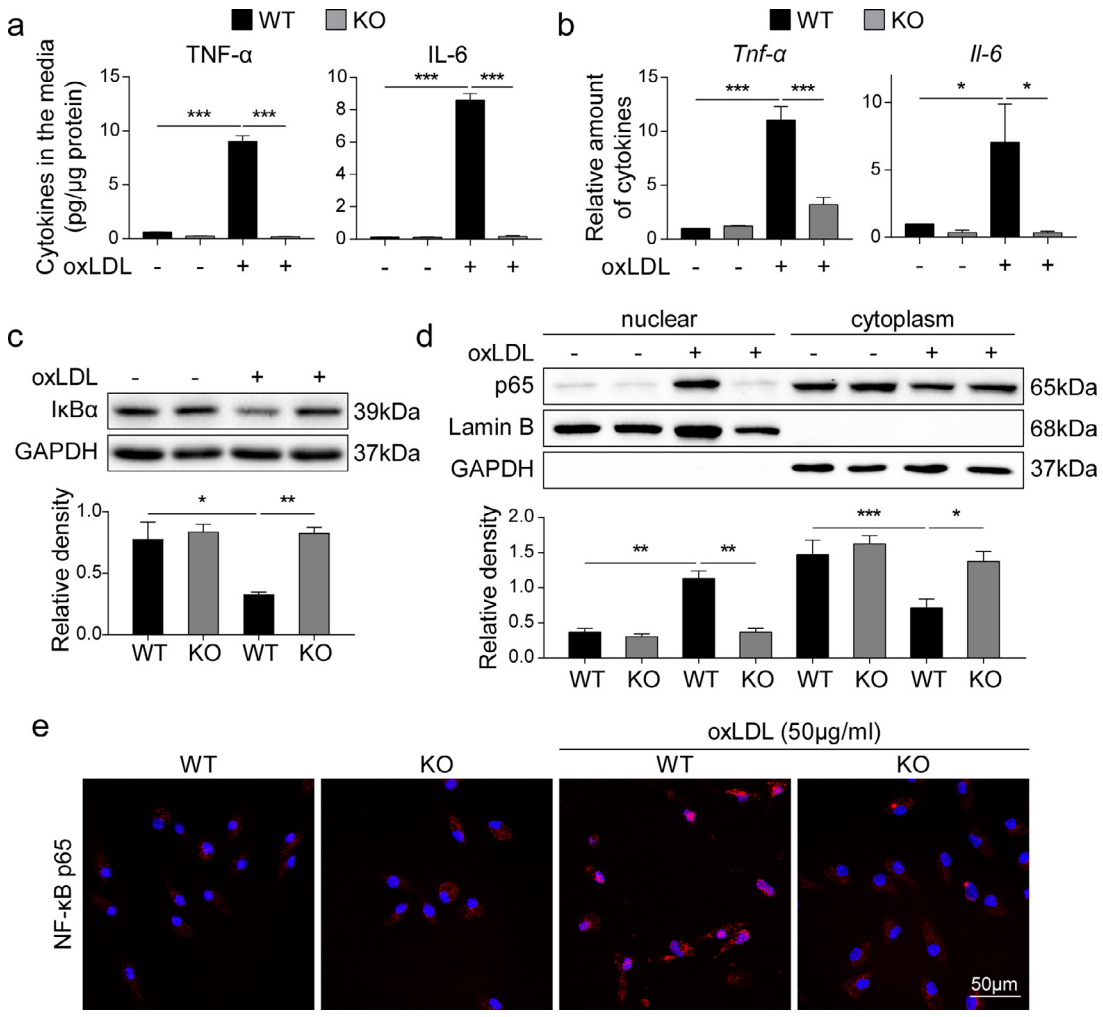

Fig. 4. MD2 mediates ox-LDL-induced proinflammatory cytokine production and NF-κB activation (**a**) Primary macrophages isolated from *Md2*$^{-/-}$ (KO) and wildtype (WT) mice were challenged with 50 μg/mL ox-LDL for 24 h. Levels of TNF-α and IL-6 cytokines in culture media were measured by ELISA and reported as pg/μg protein [*n* = 6]. (**b**) mRNA levels of *Tnf-α* and *Il-6* in macrophages isolated from KO and WT mice. Cells were exposed to 50 μg/mL ox-LDL for 6 h [*n* = 4]. (**c**) Levels of IκB in the primary macrophages exposed to 50 μg/mL ox-LDL for 30 min. GAPDH was used as loading control. Lower panel showing densitometric quantification [*n* = 4]. (**d**) Immunoblot detection of NF-κB p65 subunit in cytosolic and nuclear fractions prepared from cells exposed to 50 μg/mL ox-LDL for 30 min. Lamin B and GAPDH were used as loading control for nuclear and cytosolic proteins, respectively. Lower panel showing densitometric quantification [*n* = 4]. (**e**) Immunofluorescence staining for NF-κB p65 subunit (red) in primary macrophages exposed to ox-LDL for 1 h. Cells were counterstained with DAPI (blue) [scale bar = 50 μm]. (For interpretation of the references to color in this figure legend, the reader is referred to the web version of this article.)

labeled ox-LDL for either short or long time period. Surprisingly, no differences were found in DiI-ox-LDL uptake between wildtype and *Md2*$^{-/-}$ macrophages (Fig. 6a). Oil Red O staining confirmed this finding and showed equal uptake of lipids in wildtype and *Md2*$^{-/-}$ macrophages (Fig. 6b). We confirmed the results by expressing MD2 in HEK-293 cells. Exposure of MD2-expressing HEK-293 cells to DiI-ox-LDL did not increase lipid uptake (Fig. 6c). Furthermore, co-transfection of HEK-293T cells with MD2 and TLR4 plasmids also did not alter ox-LDL uptake (Fig. 6c). These results show that MD2 is not involved in ox-LDL uptake. Conversely, we examined whether inhibiting uptake of ox-LDL alters oxLDL-induced MD2-TLR4 complex formation. Moreover, we reasoned that inhibiting lipid uptake would potentially increase extracellular level of ox-LDL and then increase the association of ox-LDL with MD2/TLR4. Our results support this idea and show that pretreatment of cells with the LDL uptake inhibitor Dynasore [19] before ox-LDL exposure enhances ApoB100-MD2-TLR4 interaction (Fig. 6d). Greater cell membrane co-localization between ApoB100 and MD2 was also observed in the presence of Dynasore (Fig. 6e, Supplementary Fig. S8b). These results show that MD2 in macrophages is not required for ox-LDL uptake. The MD2/TLR4 inflammatory activation and ox-LDL uptake seems to be independent pathways.

3.8. Pharmacological inhibition of MD2 prevents atherosclerotic lesion development

Our last objective was to test whether pharmacological inhibition of MD2 prevents inflammatory macrophage activation and atherosclerosis development. For these studies, we utilized a small molecule inhibitor of MD2, namely L6H9, which binds directly to MD2 and prevents MD2-mediated TLR4 activation [39]. The anti-inflammatory activity of L6H9 was confirmed in ox-LDL-stimulated macrophages. L6H9 dose-dependently prevented ox-LDL-induced TNF-α and IL-6 production in wildtype primary macrophages (Supplementary Fig. S9a). Associated with this suppression of cytokines, we noted reduced nuclear localization of NF-κB p65 subunit and increased IκBα levels in primary macrophages treated with L6H9 (Supplementary Fig. S9b and c). Furthermore, NF-κB reporter activity was supressed by L6H9 treatment in RAW264.7 macrophage cells line exposed to ox-LDL (Supplementary Fig. S9d). We treated *Apoe*$^{-/-}$ mice with L6H9 and determined whether MD2 inhibition mimics the results obtained from *Apoe*$^{-/-}$*Md2*$^{-/-}$ mice. L6H9 treatment of *Apoe*$^{-/-}$ mice fed a HFD did not alter body weight gain (Supplementary Figure S10a) or serum lipid profile (Supplementary Fig. S10b). Unlike *Apoe*$^{-/-}$*Md2*$^{-/-}$ mice, treatment of *Apoe*$^{-/-}$ mice with L6H9 did not

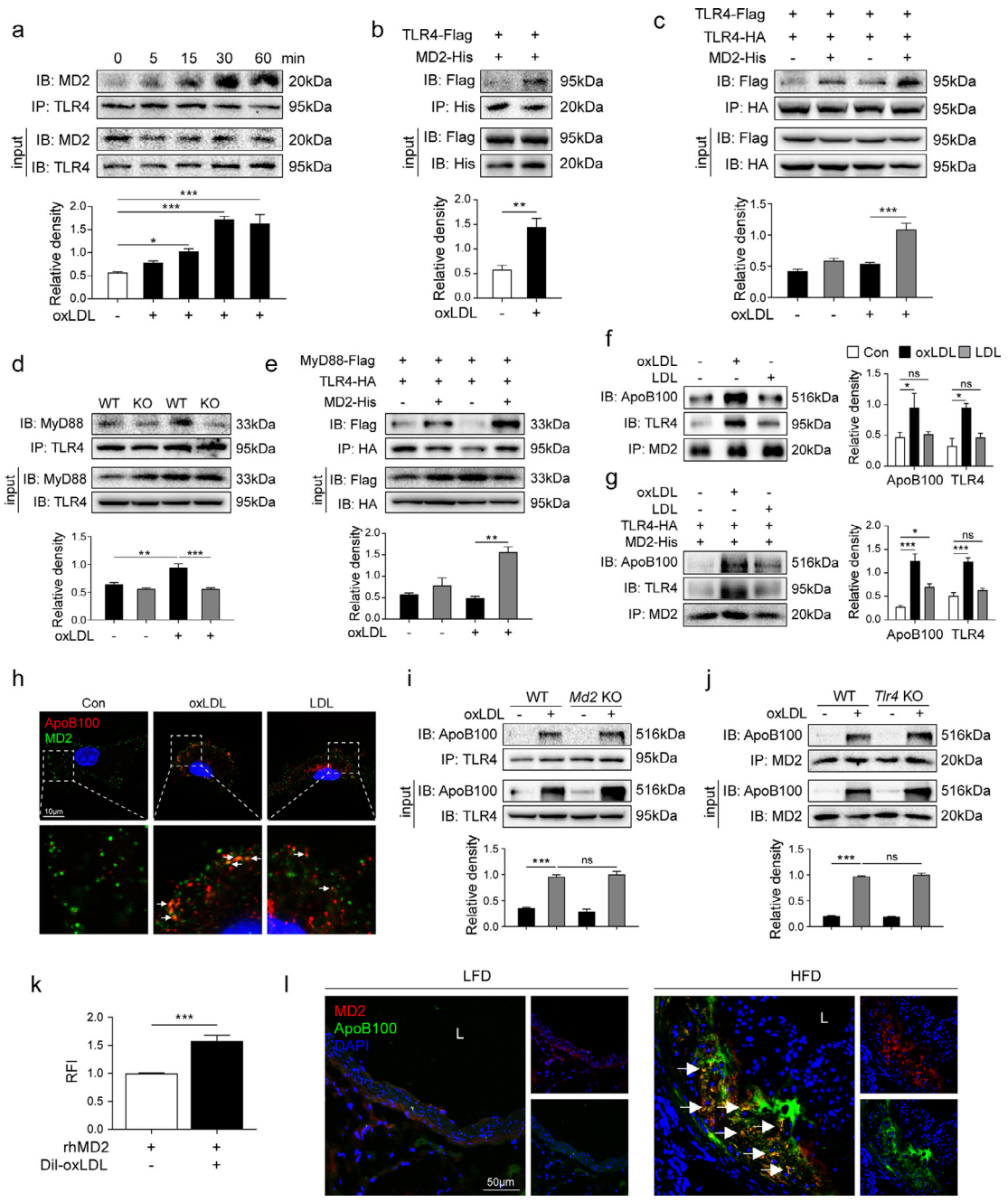

Fig. 5. MD2 is essential for ox-LDL-induced TLR4 dimerization and activation via direct interaction with ox-LDL (**a**) Macrophages from wildtype mice were incubated with 50 μg/mL ox-LDL for indicated time periods. TLR4 was immunoprecipitated (IP) and MD2 was detected by immunoblotting (IB). Lower panel showing the densitometric quantification of MD2-TLR4 association [n = 4]. (**b**) Interaction between MD2 and TLR4 was confirmed by co-immunoprecipitation assay in HEK-293T cells transfected with MD2-His and TLR4-Flag expressing plasmids. Lower panel showing the densitometric quantification [n = 4]. (**c**) Dimerization of TLR4 was assessed by co-immunoprecipitation assay in HEK-293T cells transfected with Flag- and HA-tagged TLR4 and His-tagged MD2 plasmids. Cells were exposed to 50 μg/mL ox-LDL for 30 min. Samples were immunoprecipitation (IP) with anti-HA followed by immunoblotting (IB) with anti-Flag. Lower panel showing the densitometric quantification. [n = 4]. (**d**) Primary macrophages from wildtype (WT) mice and MD2$^{-/-}$ mice (KO) were incubated with 50 μg/mL ox-LDL for 30 min. TLR4 was immunoprecipitated (IP) and MyD88 was detected by immunoblotting (IB). Lower panel showing the densitometric quantification [n = 4]. (**e**) Interaction between MyD88 and TLR4 was detected by co-immunoprecipitation assay in HEK-293T cells transfected with TLR4-HA, MyD88-Flag, and MD2-His expressing plasmids. Cells were treated with or without 50 μg/mL ox-LDL for 30 min. Lower panel showing the densitometric quantification [n = 3]. (**f**) Macrophages isolated from wildtype mice were exposed to 50 μg/mL ox-LDL or LDL for 30 min. Interaction between ApoB100, MD2, and TLR4 was assessed by co-immunoprecipitation. Right panel showing the densitometric quantification [n = 3]. (**g**) Interaction between ApoB100, MD2, and TLR4 was detected by co-immunoprecipitation in HEK-293T cells transfected with TLR4-HA and MD2-His expressing plasmids. Cells were treated with or without 50 μg/mL ox-LDL for 30 min. Right panel showing the densitometric quantification [n = 4]. (**h**) Primary macrophages were treated with 50 μg/mL ox-LDL or LDL, and then were stained for MD2 (green) and ApoB100 (red). DAPI (blue) was used to counterstain. Lower panels show higher magnification. (**i**) Macrophages isolated from wildtype (WT) and *Md2*$^{-/-}$ (*Md2*KO) mice were incubated with 50 μg/mL ox-LDL for 30 min. Interaction between TLR4 and ApoB100 was assessed by co-immunoprecipitation. Lower panel showing the densitometric quantification [n = 3] (**j**) Macrophages isolated from WT and *Tlr4*$^{-/-}$ (*Tlr4*KO) mice were incubated with 50 μg/mL ox-LDL for 30 min. Interaction between MD2 and ApoB100 was assessed by co-immunoprecipitation. Lower panel showing the densitometric quantification [n = 3]. (**k**) The interaction between MD2 and ox-LDL was determined using a cell-free assay. rhMD2 was immobilized and Dil-labeled ox-LDL was added. Binding was determined by relative fluorescence intensity (RFI), normalized to blanks without rhMD2 immobilization [n = 4]. (**l**) Representative immunofluorescence staining of MD2 (red) and ApoB100 (green) in aortic sinus of *Apoe*$^{-/-}$ mice maintained on HFD. Tissues were counterstained with DAPI (blue) [scale bar = 50 μm]. (For interpretation of the references to color in this figure legend, the reader is referred to the web version of this article.)

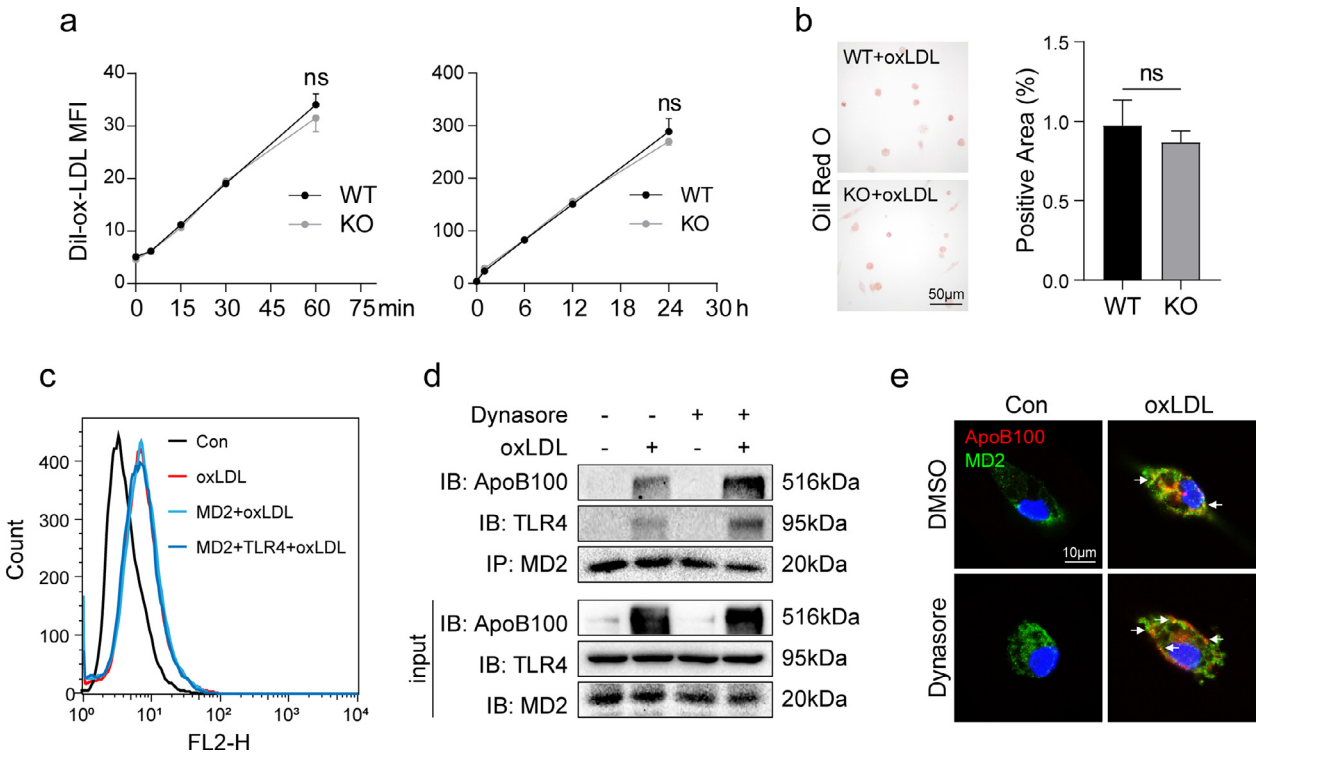

Fig. 6. MD2 in macrophages is not required for ox-LDL uptake (**a**) Primary macrophages isolated from widetype (WT) and *Md2*$^{-/-}$ (KO) mice were incubated with 50 μg/mL DiI-labeled ox-LDL for indicated time periods. DiI-ox-LDL uptake was detected as mean fluorescence intensity by flow cytometry [n = 4]. (**b**) Oil Red O staining of WT and KO macrophages incubated with 50 μg/mL ox-LDL for 24 h. Right panel showing quantification of area highlighted by Oil Red O staining [n = 4]. (**c**) HEK-293T cells transfected with MD2-His-plasmid alone or co-transfected with MD2-His-and TLR4-HA plasmids were cultured with 50 μg/mL DiI-labeled ox-LDL for 30 min. DiI-ox-LDL uptake was detected by flow cytometry. Flow histograms showing mean fluorescence intensity (MFI) values. (**d**) The interaction between ApoB100, MD2, and TLR4 was assessed by co-immunoprecipitation in macrophages from wildtype mice. Cells were pretreated with or without LDL-uptake inhibitor Dynasore at 80 μM for 1 h prior to exposure of cells to 50 μg/mL ox-LDL for 30 min. (**e**) Immunofluorescence staining of macrophages from wildtype mice for MD2 (green) and ApoB100 (red). Cells were treated as indicated in panel D. Cells were counterstained with DAPI (blue). (For interpretation of the references to color in this figure legend, the reader is referred to the web version of this article.)

increase HDL levels. However, we did find reduced aortic plaques in mice treated with L6H9 (Fig. 7a and b). L6H9 also reduced α-SMA immunoreactivity in aortas (Fig. 7c). Similar to results obtained from *Md2*$^{-/-}$ mice, pharmacological inhibition of MD2 had no effect on HFD-induced connective tissue expansion in the aortas, as evidenced by Masson's Trichrome staining (Fig. 7d). Analysis of circulating inflammatory cytokines showed that L6H9 reduces the amounts of both TNF-α and IL-6 in mice fed a HFD (Fig. 7e). Transcript levels of *Tnf-α*, *Il-6*, *Il-1β*, *Icam-1*, and *Vcam-1* were also reduced in aortic sinus of mice upon treatment with L6H9 (Fig. 7f). Consistent with these observations, CD68 immunoreactivity of aortic sinus tissues was decreased in mice treated with L6H9 (Fig. 7g and h). Overall, these data confirm that inhibition of MD2 prevents atherosclerotic injuries through suppression of macrophage infiltration and inflammation.

4. Discussion

The key findings of our study include the demonstration that macrophage-derived MD2 is required for atherosclerotic plaque development in high-fat diet-induced *Apoe*$^{-/-}$ mouse model. We show that MD2 deficiency or inhibition prevents macrophage infiltration and inflammatory cytokine production in atherosclerotic mice. Reconstitution of *Apoe*$^{-/-}$ mice with marrow cells harvested from *Apoe*$^{-/-}$*Md2*$^{-/-}$ mice showed that macrophage-expressed MD2 was the driver in cell activation and initiation of inflammatory injuries in aortas. Mechanistically, we show that MD2 does not alter ox-LDL uptake by macrophages but is required for TLR4 activation and inflammation via directly binding to ox-LDL triggering MD2/TLR4 complex formation and TLR4-MyD88-NFκB pro-inflammatory cascade. Collectively, these results shed new light on the role of MD2 in atherosclerosis and provide a mechanistic basis for ox-LDL-induced inflammatory responses (summarized in Fig. 8).

TLR4 activation in atherosclerosis is not a new concept [40]. Studies have shown that *Apoe*$^{-/-}$ mice deficient in TLR4 are protected against developing atherosclerotic lesions [13,14]. This protection was found to be associated with significantly reduced macrophage levels and inflammatory responses in the lesions. Blocking TLR4 also reduces the secretion of interleukins (1β, 6, and 8) [12]. Furthermore, the deficiency or inhibition of MyD88, a direct downstream protein of TLR4, also attenuated atherosclerosis through inhibiting inflammation [41,42]. Here, we showed that global or hematopoietic cell knockout of MD2 prevented atherosclerosis in mice, which was associated with reduced inflammation and macrophage infiltration in atherosclerotic lesions. These findings clearly show that MD2-TLR4 signaling is involved in at least the early inflammatory stage of atherosclerosis. However, the mechanisms by which TLR4 is activated in atherosclerosis are far from established. The interaction between activated monocytes and ox-LDL is critical to the development of atherosclerosis. The likely mechanism entails oxidized lipoproteins possibly serving as danger-associated molecular patterns for TLR4 [43]. Based on our studies, the recognition and activation of TLR4 by ox-LDL requires MD2, much like LPS, the prototypical TLR4 ligand. We found that ox-LDL increased the association between MD2 and TLR4 in macrophages and thus, recruited MyD88 and activated NF-κB to elevate inflammatory cytokine expression. Therefore, our studies provide novel insight into the mechanisms by which ox-LDL induces TLR4 pro-inflammatory signaling in macrophages and feeds atherogenesis.

As an accessory protein, MD2 helps TLR4 to link the ligands (*e.g.* LPS [44] and saturated fatty acid [39]), leading to inflammatory

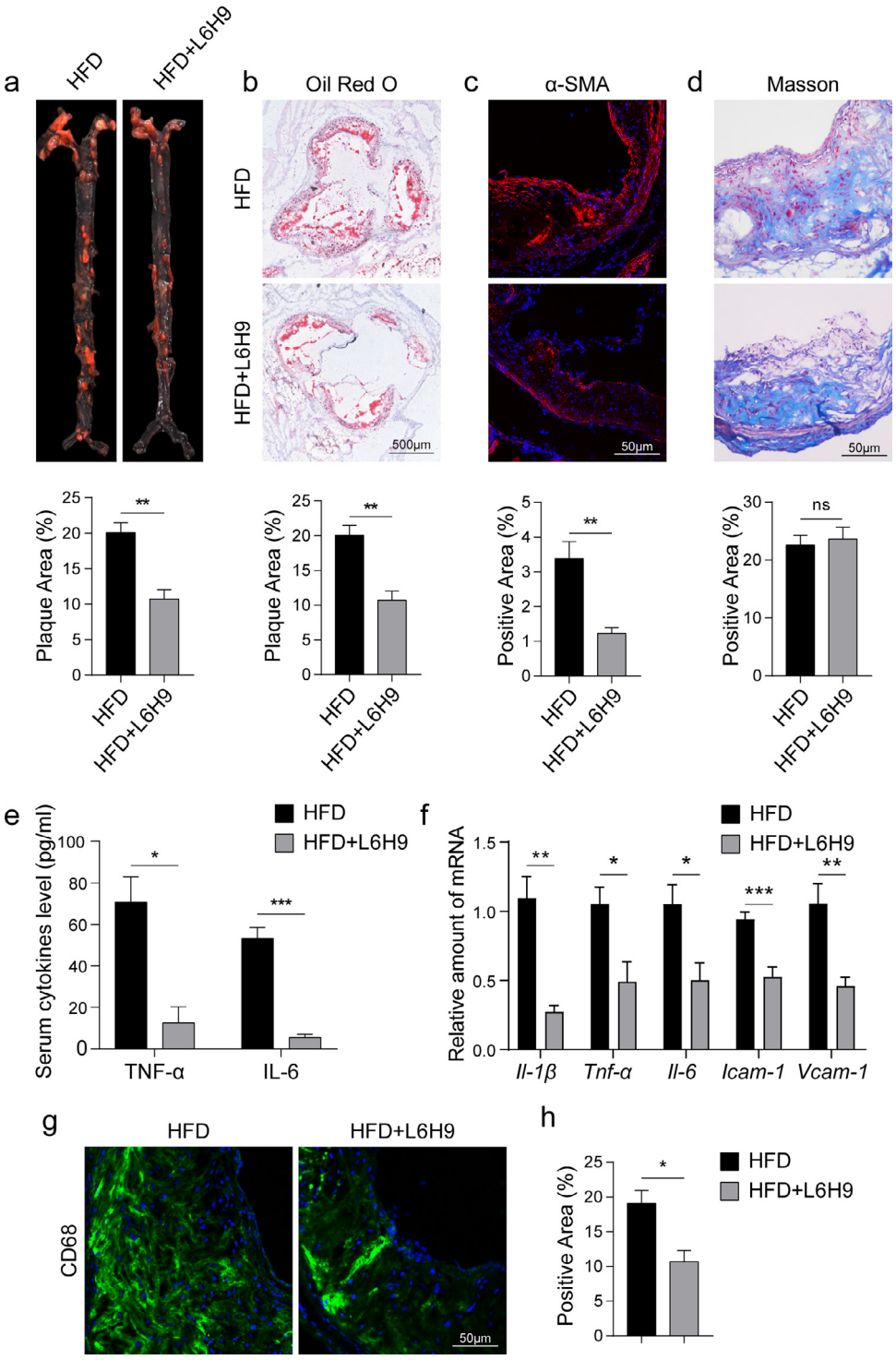

Fig. 7. Pharmacological inhibition of MD2 by L6H9 reduces the development of atherosclerosis and inflammation in mice. (**a**) En face Oil Red O staining of aortas. *Apoe*$^{-/-}$ mice maintained on HFD were treated with 10 mg/kg L6H9 every other day. Oil Red O staining highlighting neutral lipids (red). Lower panel showing quantification of plaque lesion area [n = 6]. (**b**) Oil Red O staining of lesion area in aortic sinus. Lower panel showing quantification of lesion area highlighted by Oil Red O staining [n = 6; scale bar = 500 μm]. (**c**) Representative images of α-SMA staining (red) of aortic sinus. Lower panel showing quantification of α-SMA staining area [n = 6; scale bar = 50 μm]. (**d**) Representative images of Masson's Trichome staining for collagen deposition. Lower panel showing quantification of fibrotic area [n = 6; scale bar = 50 μm]. (**e**) Serum levels of pro-inflammatory cytokines TNF-α and IL-6 [n = 6]. (**f**) Real-time qPCR assay shows the levels of mRNA of proinflammatory cytokines (*Il-1β, Tnf-α, Il-6*) and adhesion molecules (*Icam-1, Vcam-1*) in aortas [n = 6]. (**g**) Representative immunofluorescence staining images for CD68 (green) in aortic sinus. Tissues were counterstained with DAPI (blue) [scale bar = 50 μm]. (**h**) Quantification of CD68-positive area in aortic sinus slices [n = 4]. (For interpretation of the references to color in this figure legend, the reader is referred to the web version of this article.)

responses. In addition, oxidized cholesterols [37] and phospholipids (ox-PL) [38], the components of ox-LDL, have been reported to bind MD2 and activate MD2/TLR4 signaling. These studies indicated that the capability of ox-LDL in inducing TLR4 activation likely resulted from its direct interaction with MD2 protein. As expected, our cell free binding assay showed that rhMD2 directly binding to ox-LDL, and a complex of ApoB100-MD2-TLR4 was observed in macrophages challenged with ox-LDL. This ApoB100-MD2/TLR4 pro-inflammatory

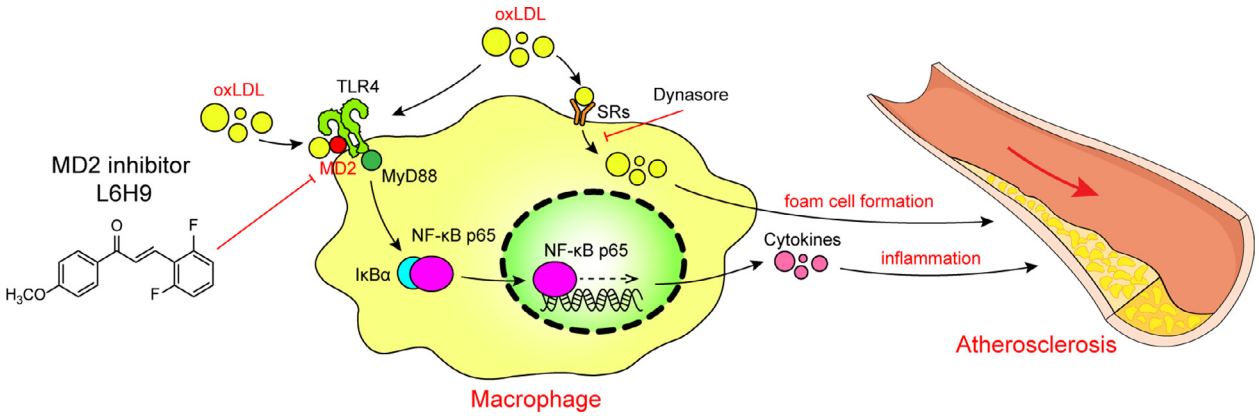

Fig. 8. Schematic illustration of the underlying mechanism of MD2 in ox-LDL-induced inflammatory responses in atherosclerosis.

cascade was not activated by unmodified LDL, which is consistent with previous evidence that ox-PL but not phospholipids in native LDL serves as DAMP that are recognized by PRRs [38,45]. Ox-LDL contains hundreds of different oxidized lipid molecules. Therefore, the discrepancy we observed in ox-LDL and LDL might be due to different oxidative status of cholesterols or phospholipids.

We found that ox-LDL-induced TLR4 activity was inhibited by MD2 deficiency, but the uptake of ox-LDL was independent on MD2/TLR4. Even though MD2 interacted with ox-LDL in a cell-free system, the mechanisms of ox-LDL uptake in macrophage are clearly separate. Importantly, we show that inhibiting ox-LDL uptake by Dynasore enhances interaction between TLR4 and MD2 in macrophages, as evidenced by increased ApoB100-MD2-TLR4 complex formation. Studies have shown that CD36 and SR-A may account for 75−90% of ox-LDL internalization by macrophages [46,47]. However, CD36 and SR-A deficiency in mice does not reduce atherosclerotic lesions [48], suggesting that compensatory detrimental mechanisms are at play. It is possible that reduced ox-LDL uptake by CD36 and SR-A deficiency increased extracellular ox-LDL level, which, on the contrary, amplifies inflammatory injuries by MD2/TLR4 signaling pathway.

We noted that whole-body knockout of MD prevented the atherosclerosis in a much stronger manner than the bone marrow chimeras (Figs. 2 and 3). The reason may be the involvement of MD2/TLR4 signaling in other cell types including stromal cells. A recent study showed that TLR4 signaling in both stromal and hematopoietic cells contribute to aortic inflammation and atherogenesis in mouse model of HFD-induced atherosclerosis [49]. TLR4 in vascular smooth *muscle* cells and endothelial cells has been also reported to mediate the inflammatory atherosclerosis [50,51]. In addition, both *Apoe*$^{-/-}$*Md2*$^{-/-}$ mice and *Apoe*$^{-/-}$ mice treated with L6H9 show no changes in fibrosis. Extracellular matrix proteins in atherosclerosis may be derived from endothelial cells, vascular smooth muscle cells, and adventitial fibroblasts. One possibility is that MD2 deficiency in these accessory cells is not required for matrix protein synthesis. Another unexpected finding of our study was the increase in serum HDL levels in HFD-fed *Apoe*$^{-/-}$*Md2*$^{-/-}$ mice. HDL has potential antiatherogenic effects and it is known to exert an anti-inflammatory activity against a wide range of inflammatory agents, including ox-LDL [52]. Thus, the increased HDL in *Apoe*$^{-/-}$*Md2*$^{-/-}$ mice may partly contribute to the anti-atherosclerosis effects of MD2 deficiency. ApoA-1, the predominant apolipoprotein of HDL, mediates cellular cholesterol efflux through an ATP-binding transporter ABCA1 in macrophages [53]. Therefore, increased HDL in *Md2*$^{-/-}$ mice may contribute to the protective effects seen in our study through regulating cholesterol efflux. Interestingly, the increase in serum HDL was not seen in HFD-fed *Apoe*$^{-/-}$ mice transplanted with *Apoe*$^{-/-}$*Md2*$^{-/-}$ marrow cells. HDL is mainly produced in the liver and intestine. This indicates that MD2 in liver cells or intestine cells may regulate the synthesis of HDL. Therefore, a potential future study may explore the HDL-regulating role and mechanism of MD2 in liver or intestine. In addition, the supplementary Fig. S10 showed that mice treated with L6H9 do not affect serum HDL level. Although L6H9 treatment seems to be another model of 'global' MD2 functional deficiency, the drug concentrations of L6H9 in liver and intestine need to be determined. This also indicates that the organ distribution data of L6H9 may be important for its pre-clinical pharmacokinetic evaluation.

In summary, we report here that TLR4-coreceptor MD2 is required for atherosclerotic plaque development in the high-fat diet-induced *Apoe*$^{-/-}$ model. Knocking out MD2 in this model shows prevention of macrophage infiltration, and inhibited production of proinflammatory cytokines. These results are recapitulated in mice treated with a MD2 inhibitor L6H9. Reconstitution of irradiated *Apoe*$^{-/-}$ mice with *Md2*$^{-/-}$ marrow cells showed that bone marrow-derived MD2 was important in initiation of inflammatory injuries. Using cultured macrophages, we also showed that MD2 did not alter ox-LDL uptake but regulated ox-LDL-induced TLR4 activation and inflammation possibly via directly interaction with ox-LDL. Therefore, our studies provide a mechanistic basis of ox-LDL-induced macrophage inflammation in atherosclerosis. Collectively, these results have shed new light on the role of MD2 in atherosclerosis and support the therapeutic potential of MD2 targeting in atherosclerosis-driven cardiovascular diseases.

Authors' contributions

This work was carried out in collaboration among all authors. Guang Liang and Weijian Huang contributed to the literature search and study design. Guang Liang and Gaojun Wu participated in the drafting of the article. Taiwei Chen, Jinfu Qian, Wu Luo, and Ke Lin carried out the experiments. Taiwei Chen, Peiren Shan, Yan Cai and Gaojun Wu revised the manuscript. Yan Cai and Gaojun Wu contributed to data collection and analysis. All authors have read and approved the final manuscript.

Declaration of Competing Interest

The authors declare that they have no conflicts of interest.

Funding sources

This work was supported by the National Key Research Project of China (2017YFA0506000), National Natural Science Foundation of China (21961142009, 81930108, 81670244, and 81700402), and Natural Science Foundation of Zhejiang Province (LY19H020004). The funders had no role in the study design, data collection, data analysis, interpretation and writing of the report.

Acknowledgment

We thank Dr. Zia Ali Khan (University of Ontario, Canada) for language editing of the manuscript.

Supplementary materials

Supplementary material associated with this article can be found in the online version at doi:10.1016/j.ebiom.2020.102706.

References

[1] Lozano R, Naghavi M, Foreman K, Lim S, Shibuya K, Aboyans V, et al. Global and regional mortality from 235 causes of death for 20 age groups in 1990 and 2010: a systematic analysis for the Global Burden of Disease Study 2010. Lancet 2012;380(9859):2095–128.
[2] Robbins JM, Webb DA, Sciamanna CN. Cardiovascular comorbidities among public health clinic patients with diabetes: the Urban Diabetics Study. BMC Public Health 2005;5:15.
[3] Libby P, Ridker PM, Maseri A. Inflammation and atherosclerosis. Circulation 2002;105(9):1135–43.
[4] Kwon GP, Schroeder JL, Amar MJ, Remaley AT, Balaban RS. Contribution of macromolecular structure to the retention of low-density lipoprotein at arterial branch points. Circulation 2008;117(22):2919–27.
[5] Hansson GK, Hermansson A. The immune system in atherosclerosis. Nat Immunol 2011;12(3):204–12.
[6] Williams KJ, Tabas I. The response-to-retention hypothesis of early atherogenesis. Arterioscler Thromb Vasc Biol. 1995;15(5):551–61.
[7] Glass CK, Witztum JL. Atherosclerosis. the road ahead. Cell 2001;104(4):503–16.
[8] Mestas J, Ley K. Monocyte-endothelial cell interactions in the development of atherosclerosis. Trends Cardiovasc. Med. 2008;18(6):228–32.
[9] Moore KJ, Tabas I. Macrophages in the pathogenesis of atherosclerosis. Cell 2011;145(3):341–55.
[10] Curtiss LK, Tobias PS. Emerging role of Toll-like receptors in atherosclerosis. J Lipid Res. 2009;50(Suppl):S340–5.
[11] Howell KW, Meng X, Fullerton DA, Jin C, Reece TB, Cleveland Jr. JC. Toll-like receptor 4 mediates oxidized LDL-induced macrophage differentiation to foam cells. J Surg Res. 2011;171(1):e27–31.
[12] Chavez-Sanchez L, Garza-Reyes MG, Espinosa-Luna JE, Chavez-Rueda K, Legorreta-Haquet MV, Blanco-Favela F. The role of TLR2, TLR4 and CD36 in macrophage activation and foam cell formation in response to oxLDL in humans. Hum Immunol. 2014;75(4):322–9.
[13] Michelsen KS, Wong MH, Shah PK, Zhang W, Yano J, Doherty TM, et al. Lack of Toll-like receptor 4 or myeloid differentiation factor 88 reduces atherosclerosis and alters plaque phenotype in mice deficient in apolipoprotein E. Proc Natl Acad Sci USA 2004;101(29):10679–84.
[14] Mullick AE, Tobias PS, Curtiss LK. Modulation of atherosclerosis in mice by Toll-like receptor 2. J Clin Investig 2005;115(11):3149–56.
[15] Stewart CR, Stuart LM, Wilkinson K, van Gils JM, Deng J, Halle A, et al. CD36 ligands promote sterile inflammation through assembly of a Toll-like receptor 4 and 6 heterodimer. Nat Immunol 2010;11(2):155–61.
[16] Cole JE, Mitra AT, Monaco C. Treating atherosclerosis: the potential of Toll-like receptors as therapeutic targets. Expert Rev Cardiovasc Ther 2010;8(11):1619–35.
[17] Newton K, Dixit VM. Signaling in innate immunity and inflammation. Cold Spring Harb Perspect Biol 2012;4(3).
[18] Takeda K, Akira S. Toll-like receptors in innate immunity. Int Immunol 2005;17(1):1–14.
[19] Preta G, Cronin JG, Sheldon IM. Dynasore - not just a dynamin inhibitor. Cell Commun Signal 2015;13:24.
[20] Girard E, Paul JL, Fournier N, Beaune P, Johannes L, Lamaze C, et al. The dynamin chemical inhibitor dynasore impairs cholesterol trafficking and sterol-sensitive genes transcription in human HeLa cells and macrophages. PLoS One 2011;6(12):e29042.
[21] Wu J, Li J, Cai Y, Pan Y, Ye F, Zhang Y, et al. Evaluation and discovery of novel synthetic chalcone derivatives as anti-inflammatory agents. J Med Chem 2011;54(23):8110–23.
[22] Wang L, Huang Z, Huang W, Chen X, Shan P, Zhong P, et al. Inhibition of epidermal growth factor receptor attenuates atherosclerosis via decreasing inflammation and oxidative stress. Sci Rep 2017;8:45917.
[23] Pan Y, Wang Y, Cai L, Cai Y, Hu J, Yu C, et al. Inhibition of high glucose-induced inflammatory response and macrophage infiltration by a novel curcumin derivative prevents renal injury in diabetic rats. Br J Pharmacol 2012;166(3):1169–82.
[24] Weber C, Zernecke A, Libby P. The multifaceted contributions of leukocyte subsets to atherosclerosis: lessons from mouse models. Nat Rev Immunol 2008;8(10):802–15.
[25] Vogel SN, Hansen CT, Rosenstreich DL. Characterization of a congenitally LPS-resistant, athymic mouse strain. J Immunol 1979;122(2):619–22.
[26] Nakashima Y, Plump AS, Raines EW, Breslow JL, Ross R. ApoE-deficient mice develop lesions of all phases of atherosclerosis throughout the arterial tree. Arterioscler Thromb 1994;14(1):133–40.
[27] Reddick RL, Zhang SH, Maeda N. Atherosclerosis in mice lacking apo E. Evaluation of lesional development and progression. Arterioscler Thromb 1994;14(1):141–7.
[28] Visintin A, Mazzoni A, Spitzer JA, Segal DM. Secreted MD-2 is a large polymeric protein that efficiently confers lipopolysaccharide sensitivity to Toll-like receptor 4. Proc Natl Acad Sci USA 2001;98(21):12156–61.
[29] Hansson GK, Robertson AK, Soderberg-Naucler C. Inflammation and atherosclerosis. Annu Rev Pathol 2006;1:297–329.
[30] Shindo A, Tanemura H, Yata K, Hamada K, Shibata M, Umeda Y, et al. Inflammatory biomarkers in atherosclerosis: pentraxin 3 can become a novel marker of plaque vulnerability. PLoS One 2014;9(6):e100045.
[31] Cominacini L, Garbin U, Pasini AF, Davoli A, Campagnola M, Contessi GB, et al. Antioxidants inhibit the expression of intercellular cell adhesion molecule-1 and vascular cell adhesion molecule-1 induced by oxidized LDL on human umbilical vein endothelial cells. Free Radic Biol Med 1997;22(1–2):117–27.
[32] Frostegard J, Haegerstrand A, Gidlund M, Nilsson J. Biologically modified LDL increases the adhesive properties of endothelial cells. Atherosclerosis 1991;90(2–3):119–26.
[33] Auron PE, Webb AC. Interleukin-1: a gene expression system regulated at multiple levels. Eur Cytokine Netw 1994;5(6):573–92.
[34] Vanden Berghe W, De Bosscher K, Boone E, Plaisance S, Haegeman G. The nuclear factor-kappaB engages CBP/p300 and histone acetyltransferase activity for transcriptional activation of the interleukin-6 gene promoter. J Biol Chem 1999;274(45):32091–8.
[35] Udalova IA, Knight JC, Vidal V, Nedospasov SA, Kwiatkowski D. Complex NF-kappaB interactions at the distal tumor necrosis factor promoter region in human monocytes. J Biol Chem 1998;273(33):21178–86.
[36] Saitoh S, Akashi S, Yamada T, Tanimura N, Kobayashi M, Konno K, et al. Lipid A antagonist, lipid IVa, is distinct from lipid A in interaction with Toll-like receptor 4 (TLR4)-MD-2 and ligand-induced TLR4 oligomerization. Int Immunol 2004;16(7):961–9.
[37] Choi SH, Kim J, Gonen A, Viriyakosol S, Miller YI. MD-2 binds cholesterol. Biochem Biophys Res Commun 2016;470(4):877–80.
[38] Mancek-Keber M, Frank-Bertoncelj M, Hafner-Bratkovic I, Smole A, Zorko M, Pirher N, et al. Toll-like receptor 4 senses oxidative stress mediated by the oxidation of phospholipids in extracellular vesicles. Sci Signal 2015;8(381):ra60.
[39] Wang Y, Qian Y, Fang Q, Zhong P, Li W, Wang L, et al. Saturated palmitic acid induces myocardial inflammatory injuries through direct binding to TLR4 accessory protein MD2. Nat Commun 2017;8:13997.
[40] Cole JE, Georgiou E, Monaco C. The expression and functions of toll-like receptors in atherosclerosis. Mediators Inflamm 2010;2010:393946.
[41] Bjorkbacka H, Kunjathoor VV, Moore KJ, Koehn S, Ordija CM, Lee MA, et al. Reduced atherosclerosis in Myd88-null mice links elevated serum cholesterol levels to activation of innate immunity signaling pathways. Nat Med 2004;10(4):416–21.
[42] Chen T, Luo W, Wu G, Wu L, Huang S, Li J, et al. A novel Myd88 inhibitor LM9 prevents atherosclerosis by regulating inflammatory responses and oxidative stress in macrophages. Toxicol Appl Pharmacol 2019;370:44–55.
[43] Miller YI. Toll-like receptors and atherosclerosis: oxidized LDL as an endogenous Toll-like receptor ligand. Future Cardiol 2005;1(6):785–92.
[44] Shimazu R, Akashi S, Ogata H, Nagai Y, Fukudome K, Miyake K, et al. MD-2, a molecule that confers lipopolysaccharide responsiveness on Toll-like receptor 4. J Exp Med 1999;189(11):1777–82.
[45] Miller YI, Shyy JY. Context-Dependent role of oxidized lipids and lipoproteins in inflammation. Trends Endocrinol Metab 2017;28(2):143–52.
[46] Collot-Teixeira S, Martin J, McDermott-Roe C, Poston R, McGregor JL. CD36 and macrophages in atherosclerosis. Cardiovasc Res 2007;75(3):468–77.
[47] Kunjathoor VV, Febbraio M, Podrez EA, Moore KJ, Andersson L, Koehn S, et al. Scavenger receptors class A-I/II and CD36 are the principal receptors responsible for the uptake of modified low density lipoprotein leading to lipid loading in macrophages. J Biol Chem 2002;277(51):49982–8.
[48] Manning-Tobin JJ, Moore KJ, Seimon TA, Bell SA, Sharuk M, Alvarez-Leite JI, et al. Loss of SR-A and CD36 activity reduces atherosclerotic lesion complexity without abrogating foam cell formation in hyperlipidemic mice. Arterioscler Thromb Vasc Biol 2009;29(1):19–26.
[49] Chen S, Shimada K, Crother TR, Erbay E, Shah PK, Arditi M. Chlamydia and lipids engage a common signaling pathway that promotes atherogenesis. J Am Coll Cardiol 2018;71(14):1553–70.
[50] Yin YW, Liao SQ, Zhang MJ, Liu Y, Li BH, Zhou Y, et al. TLR4-mediated inflammation promotes foam cell formation of vascular smooth muscle cell by upregulating ACAT1 expression. Cell Death Dis 2014;5:e1574.
[51] Qu D, Wang L, Huo M, Song W, Lau CW, Xu J, et al. Focal TLR4 activation mediates disturbed flow-induced endothelial inflammation. Cardiovasc Res 2020;116(1):226–36.
[52] Watson AD, Berliner JA, Hama SY, La Du BN, Faull KF, Fogelman AM, et al. Protective effect of high density lipoprotein associated paraoxonase. Inhibition of the biological activity of minimally oxidized low density lipoprotein. J Clin Investig 1995;96(6):2882–91.
[53] Tang C, Liu Y, Kessler PS, Vaughan AM, Oram JF. The macrophage cholesterol exporter ABCA1 functions as an anti-inflammatory receptor. J Biol Chem 2009;284(47):32336–43.